AMERICAN SOCIETY FOR MICROBIOLOGY | Antimicrobial Agents and Chemotherapy®

ANTIVIRAL AGENTS

# Modulation of Monocyte Activation and Function during Direct Antiviral Agent Treatment in Patients Coinfected with HIV and Hepatitis C Virus

**Rebeca S. De Pablo-Bernal,[a] M. Reyes Jimenez-Leon,[a] Laura Tarancon-Diez,[a]* Alicia Gutierrez-Valencia,[a] Ana Serna-Gallego,[a] Maria Trujillo-Rodriguez,[a] Ana I. Alvarez-Rios,[b] Yusnelkis Milanes-Guisado,[a] Nuria Espinosa,[a] Cristina Roca-Oporto,[a] Pompeyo Viciana,[a] Luis F. Lopez-Cortes,[a] Ezequiel Ruiz-Mateos[a]**

[a]Clinical Unit of Infectious Diseases, Microbiology and Preventive Medicine, Institute of Biomedicine of Seville (IBiS), Virgen del Rocío University Hospital, CSIC, University of Seville, Seville, Spain

[b]Department of Clinical Biochemistry, Virgen del Rocío University Hospital, CSIC, University of Seville, Seville, Spain

Rebeca S. De Pablo-Bernal and M. Reyes Jimenez-Leon contributed equally to this work. Rebeca S. De Pablo-Bernal is listed first because she did all the experiments.

**ABSTRACT** The activation phenotypes and functional changes in monocyte subsets during hepatitis C virus (HCV) elimination in HIV/HCV-coinfected patients were evaluated. Twenty-two HIV/HCV-coinfected patients on suppressive combination antiretroviral treatment (cART) achieving HCV elimination after direct-acting antiviral (DAA) therapy and 10 HIV-monoinfected patients were included. The activation phenotype (10 markers) and polyfunctionality (intracellular interleukin-1$\alpha$ [IL-1$\alpha$], IL-1$\beta$, IL-6, IL-8, tumor necrosis factor alpha [TNF-$\alpha$], and IL-10 production) in three monocyte subsets (classical, intermediate, and nonclassical) were evaluated by flow cytometry before and at the end of treatment. Cell-associated HIV DNA levels were assayed by droplet digital PCR. After HCV clearance, there was a significant increase in classical monocyte and decreases in intermediate and nonclassical monocyte levels. The levels of the activation markers CD49d, CD40, and CX3CR1 were decreased after treatment in the monocyte subsets, reaching the levels in HIV-monoinfected patients. After lipopolysaccharide (LPS) stimulation, although polyfunctionality significantly decreased in intermediate and nonclassical monocytes, some combinations, such as the IL-1$\alpha^-$ (IL-1$\alpha$-negative) IL-1$\beta^-$ IL-6$^+$ (IL-6-producing) IL-8$^-$ TNF-$\alpha^-$ IL-10$^-$ combination, were remarkably increased at the end of treatment compared to the control group. Cell-associated HIV DNA levels correlated with activation markers before but not after treatment. HCV clearance after DAA treatment in patients on cART exerts an anti-inflammatory profile on monocyte subsets, activation phenotypes, and polyfunctionality. However, there is not a complete normalization compared with HIV-monoinfected patients.

**KEYWORDS** DAAs, HCV, HIV, activation, cell-associated DNA, inflammation, monocyte, polyfunctionality, reservoir

The arrival of direct-acting antivirals (DAAs) dramatically changed the landscape of hepatitis C virus (HCV) treatment, with most trials demonstrating the chance of curing almost all patients across all genotypes and special populations. Efficacy rates of HCV treatment are demonstrated to be nearly identical between HCV-monoinfected and HIV/HCV-coinfected patients (1). HCV in HIV-infected patients confers higher rates of liver fibrosis, higher viral loads, and higher rates of hepatic decompensation (2). In HIV disease, immune activation and specifically monocyte activation are associated with a chronic inflammatory systemic status and the development of non-AIDS-related events (3, 4). In addition, HCV coinfection is associated with extrahepatic effects such

**Citation** De Pablo-Bernal RS, Jimenez-Leon MR, Tarancon-Diez L, Gutierrez-Valencia A, Serna-Gallego A, Trujillo-Rodriguez M, Alvarez-Rios AI, Milanes-Guisado Y, Espinosa N, Roca-Oporto C, Viciana P, Lopez-Cortes LF, Ruiz-Mateos E. 2020. Modulation of monocyte activation and function during direct antiviral agent treatment in patients coinfected with HIV and hepatitis C virus. Antimicrob Agents Chemother 64:e00773-20. https://doi.org/10.1128/AAC.00773-20.



Address correspondence to Ezequiel Ruiz-Mateos, ezequiel.ruizmateos@gmail.com.

* Present address: Laura Tarancon-Diez, Sección Inmunologia, Laboratory InmunoBiología Molecular, Hospital General Universitario Gregorio Marañón, Instituto de Investigación Sanitaria del Gregorio Marañón, Madrid, Spain.

**Received** 20 April 2020
**Returned for modification** 13 May 2020
**Accepted** 15 June 2020
**Accepted manuscript posted online** 22 June 2020
**Published** 20 August 2020

**TABLE 1** Characteristics of the study subjects[a]

| Characteristic | Value for group | | | *P* value for HCV/HIV BL vs ET[b] | *P* value for HCV/HIV ET vs HIV control group[c] |
|---|---|---|---|---|---|
| | HCV/HIV BL ($n = 22$) | HCV/HIV ET ($n = 22$) | HIV control group ($n = 10$) | | |
| No. of males (%) | 55 | 55 | 100 | NA | **0.010** |
| Median age (yr) (IQR) | 47 (44–51) | 47 (44–51) | 45 (37–49) | NA | 0.176 |
| Median CD4 nadir count (cells/$\mu$l) (IQR) | 172 (50–393) | 172 (50–393) | 297 (148–429) | 1 | 0.190 |
| Median $CD4^+$ T cell count (cells/$\mu$l) (IQR) | 671 (446–957) | 964 (678–1,112) | 823 (649–1,203) | 0.117 | 0.946 |
| Median $CD8^+$ T cell count (cells/$\mu$l) (IQR) | 1,038 (607–1,310) | 1,088 (796–1,549) | 1,169 (983–1,597) | 0.327 | 0.588 |
| Median ratio of $CD4^+$ to $CD8^+$ T cells (IQR) | 0.72 (0.45–0.99) | 0.86 (0.49–1.09) | 0.76 (0.57–0.89) | 0.983 | 0.436 |
| Median HIV RNA level ($log_{10}$ copies/ml) (IQR) | 1.3 (1.3–1.3) | 1.3 (1.3–1.3) | 1.3 (1.3–1.3) | 1 | 1 |
| Median HCV RNA level ($log_{10}$ copies/ml) (IQR) | 6.8 (6.2–7.2) | 1 (1–1) | NA | **0.020** | NA |
| % of patients with HCV genotype 1 | 77.8 | NA | NA | NA | NA |
| % of patients at fibrosis stage | | | | | |
| 0–1 | 44.4 | NA | NA | NA | NA |
| 2 | 44.4 | NA | NA | NA | NA |
| 3 | 5.5 | NA | NA | NA | NA |
| 4 | 5.5 | NA | NA | NA | NA |
| % of patients with cirrhosis | 5.5 | NA | NA | NA | NA |

[a]Categorical variables are expressed as percentages, and continuous variables are expressed as medians (interquartile ranges [IQR]). NA, not applicable. *P* values $<0.05$ are shown in bold.
[b]A Wilcoxon test was used to compare variables before treatment (baseline [BL]) and after treatment (end of therapy [ET]).
[c]A chi-square test and a Mann-Whitney U test were used to compare categorical and continuous variables, respectively, between the ET and the HIV-monoinfected control groups.

as cardiovascular events in HIV infection (5). For these reasons, it is important to know to what extent HCV elimination reduces monocyte activation in people living with HIV.

Monocytes include three subsets: classical monocytes ($CD14^{++}$ $CD16^-$), intermediate monocytes ($CD14^{++}$ $CD16^+$), and nonclassical monocytes ($CD14^{dim}$ $CD16^{++}$) (6). Intermediate and nonclassical monocytes have proinflammatory profiles that have been associated with cardiovascular risk and events in the general population and in people living with HIV on suppressive combination antiretroviral treatment (cART) (7, 8). This monocyte dysfunction is characterized mainly by high levels of interleukin-6 (IL-6)- and IL-10-producing monocytes (9). In addition, some studies support the hypothesis that HIV-related monocyte activation can contribute to accelerated liver fibrogenesis in HIV/HCV-coinfected patients (10). We previously found that the eradication of HCV infection in HIV/HCV-coinfected patients results in significant decreases not only in T cell activation but also in the levels of microbial translocation markers, such as lipopolysaccharide (LPS); soluble CD14 (sCD14), a marker of monocyte activation; sCD163, a marker of macrophage and liver inflammation; and D-dimers, a marker of coagulopathy. Importantly, the levels of proviral HIV DNA were also diminished after DAA treatment (11). While in HCV-monoinfected patients, changes in the frequencies of monocyte subsets have been observed (12, 13), little is known about the effect of DAAs on monocyte subset redistribution, activation, and function. Thus, the aim of this study was to evaluate the phenotype and functional changes in the three monocyte subsets during HCV eradication in HIV/HCV-coinfected patients.

(Parts of these results were presented at the 19th SAEI meeting as an oral presentation and at the 10th GESIDA national meeting as a poster presentation.)

## RESULTS

**Characteristics of the study subjects.** Twenty-two HIV/HCV-coinfected and 10 HIV-monoinfected patients matched by age and T cell levels were included. The general characteristics of the participants are summarized in Table 1. All patients were on suppressive cART with undetectable viral loads. HIV/HCV-coinfected patients completed the 12-week course of treatment with DAAs and achieved a sustained virological response (SVR). After treatment, the studied characteristics were similar to those of the control group. However, all HIV-monoinfected patients were males, compared to 54.54% in the HIV/HCV-coinfected group.

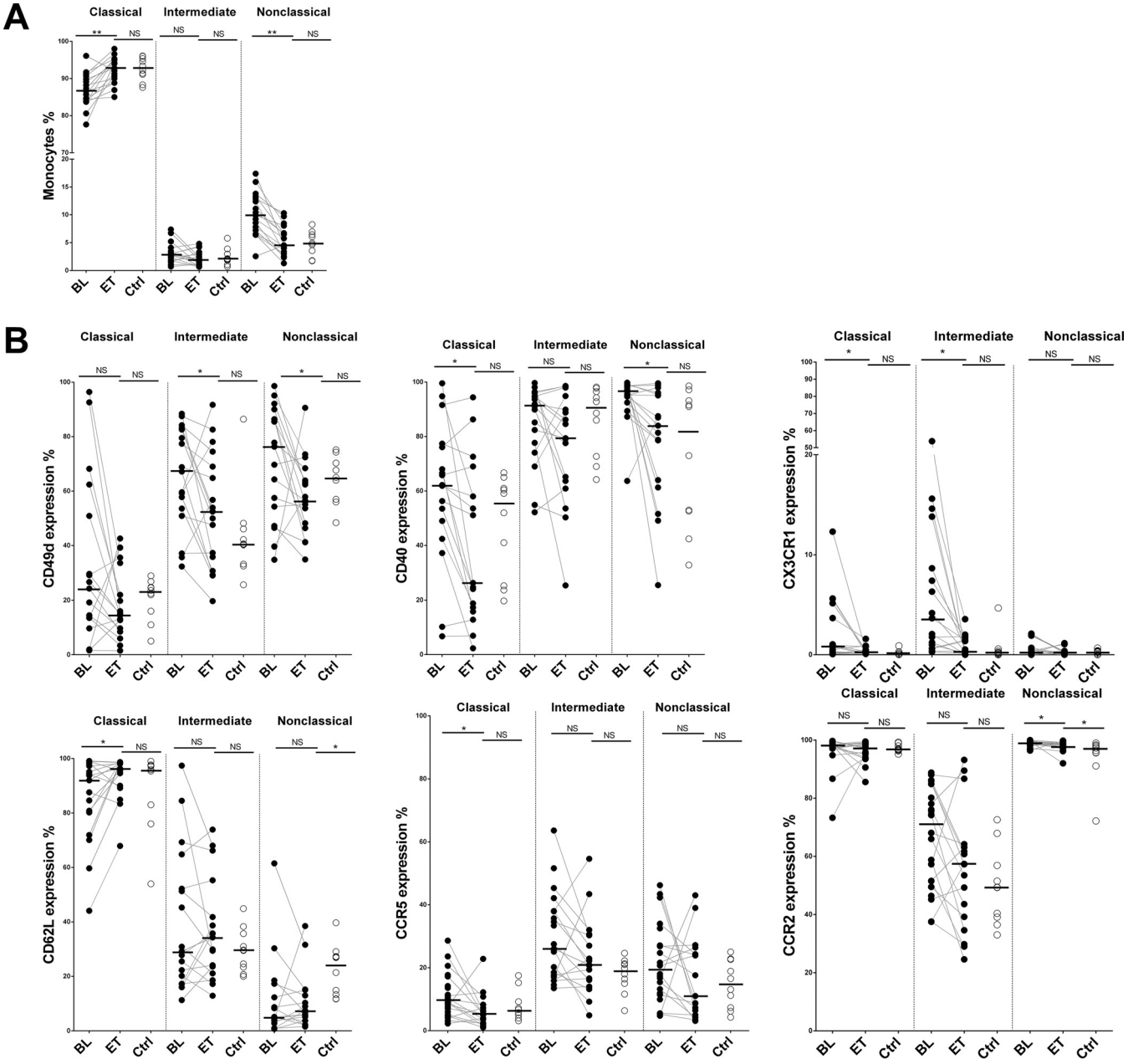


**FIG 1** HCV clearance reduces the activated phenotype of monocytes. (A) Dynamic changes in the frequencies of monocyte subsets. (B) Percentages of surface expression of activation markers among HIV/HCV-coinfected patients at baseline (BL) and at the end of treatment (ET) and the HIV-monoinfected control group (Ctrl). The Wilcoxon test was used to compare HIV/HCV-coinfected patients at baseline and at the end of treatment. The Mann-Whitney U test was used to compare HIV/HCV-coinfected patients and the HIV-monoinfected patient control group. *, $P < 0.05$; **, $P < 0.001$; NS, not significant.

**Monocyte activation markers from HIV/HCV-coinfected patients are decreased after HCV eradication.** After HCV clearance, there were significant increases in the levels of classical monocytes ($P = 0.0003$) and decreases in the levels of intermediate and nonclassical monocytes ($P = 0.19$ and $P = 0.0001$, respectively) (Fig. 1A). Integrin CD49d expression was decreased in the intermediate and nonclassical monocyte subsets after treatment (Fig. 1B). In addition, decreases of the activation and cell adhesion markers CD40 (classical and nonclassical subsets [$P = 0.004$ and $P = 0.006$, respectively]), CX3CR1 (classical and intermediate subsets [$P = 0.009$ and $P = 0.001$, respectively]), and CCR5 (classical subset [$P = 0.017$]) were also observed after treatment. After therapy, the levels of all these markers (CD49d, CD40, CX3CR1, and CCR5)

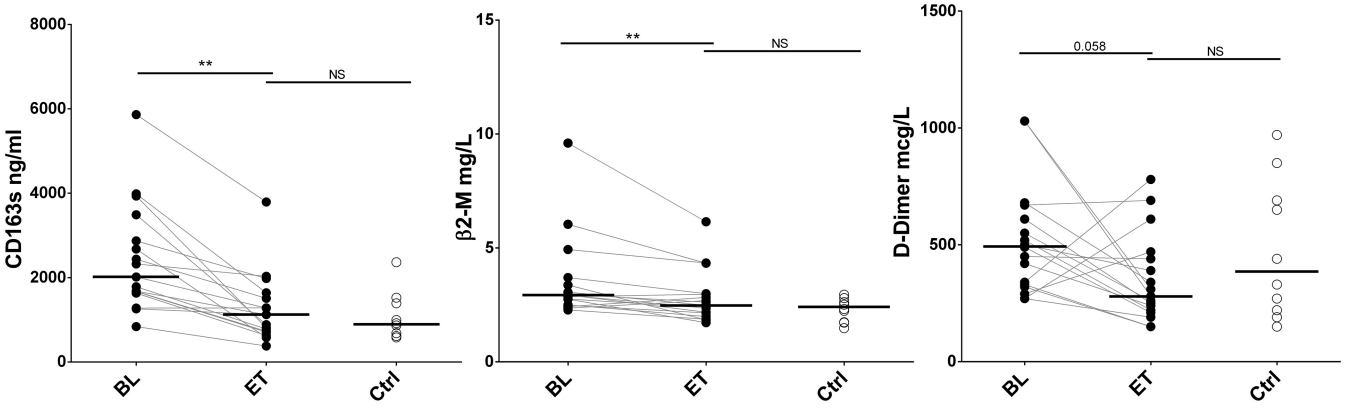


**FIG 2** Effect of DAAs on the levels of soluble biomarkers. sCD163, $\beta$2-microglobulin ($\beta$2-M), and D-dimer levels were reduced after DAA therapy. The Wilcoxon test was used to compare HIV/HCV-coinfected patients at baseline (BL) and at the end of treatment (ET). The Mann-Whitney U test was used to compare HIV/HCV-coinfected patients and the HIV-monoinfected patient control group (Ctrl). **, $P < 0.001$.

in the different subsets were similar to those found in the HIV-monoinfected control group (Fig. 1B). The expression of CD62L, implicated in homing, cell adhesion, and migration, increased ($P = 0.04$) to levels comparable to those in the monoinfected subjects for the classical subset after treatment. However, the expression of CD62L in the nonclassical subset did not reach the levels of the control group (Fig. 1B). CD62L is responsible for monocyte rolling and adhesion to endothelial cells. The downregulation of CD62L may promote atherosclerotic plaque formation and other inflammatory diseases (14, 15). CCR2 expression was decreased in nonclassical subsets but remained elevated compared to the levels in the HIV control group (Fig. 1B). High levels of CCR5, CCR2, and CD49d were previously observed in HIV-infected patients at least 1 year prior to a cardiovascular disease (CVD) event (15). Finally, we did not find differences in the percentages of the markers CD11b, Toll-like receptor 4 (TRL4), and CD163 either throughout the follow-up or compared to the control group, with the exception of CD163 in the intermediate subset, with lower levels than those in the control group (see Fig. S1A in the supplemental material). The gating strategy for monocyte subsets and activation markers is shown in Fig. S1B.

The same trends were reproduced in a confirmatory cohort ($n = 18$) of subjects with lower nadir counts and higher levels of cirrhosis (Table S1), in this case with frozen samples and markers that can be assayed in this type of material (Fig. S2).

***β*2-Microglobulin and soluble CD163 levels are decreased after HCV eradication.** sCD163 receptor and $\beta$2-microglobulin ($\beta$2M) levels decreased after treatment, reaching the levels in the HIV-monoinfected group. We also observed a trend toward decreases in the levels of the coagulation biomarker D-dimer, with these levels not being different from those in the HIV-monoinfected control group at the end of treatment (Fig. 2). We did not observe differences in the levels of high-sensitivity C-reactive protein (hsCRP), IL-6, and tumor necrosis factor alpha (TNF-$\alpha$) after HCV clearance, and these levels were similar to those in the HIV-monoinfected control group (Fig. S3).

**Single-cytokine production by monocytes after LPS stimulation.** We analyzed single-cytokine (IL-1$\alpha$, IL-1$\beta$, IL-6, IL-8, IL-10, and TNF-$\alpha$) production in response to LPS (TLR4 agonist) by the three monocyte subsets (Fig. 3 and Fig. S1B). After HCV eradication, there were no differences in IL-1$\alpha$ and IL-1$\beta$ expression compared to the HIV-monoinfected control group for all monocyte subsets. On the other hand, there were no differences in IL-6, IL-8, and IL-10 production in classical monocytes after HCV eradication, and the levels remained elevated compared to those in the HIV-monoinfected control group. IL-8 and TNF-$\alpha$ expression levels also remained elevated in the intermediate subset, and the same occurred for IL-6 and TNF-$\alpha$ in nonclassical monocytes after HCV eradication compared to the HIV-monoinfected control group

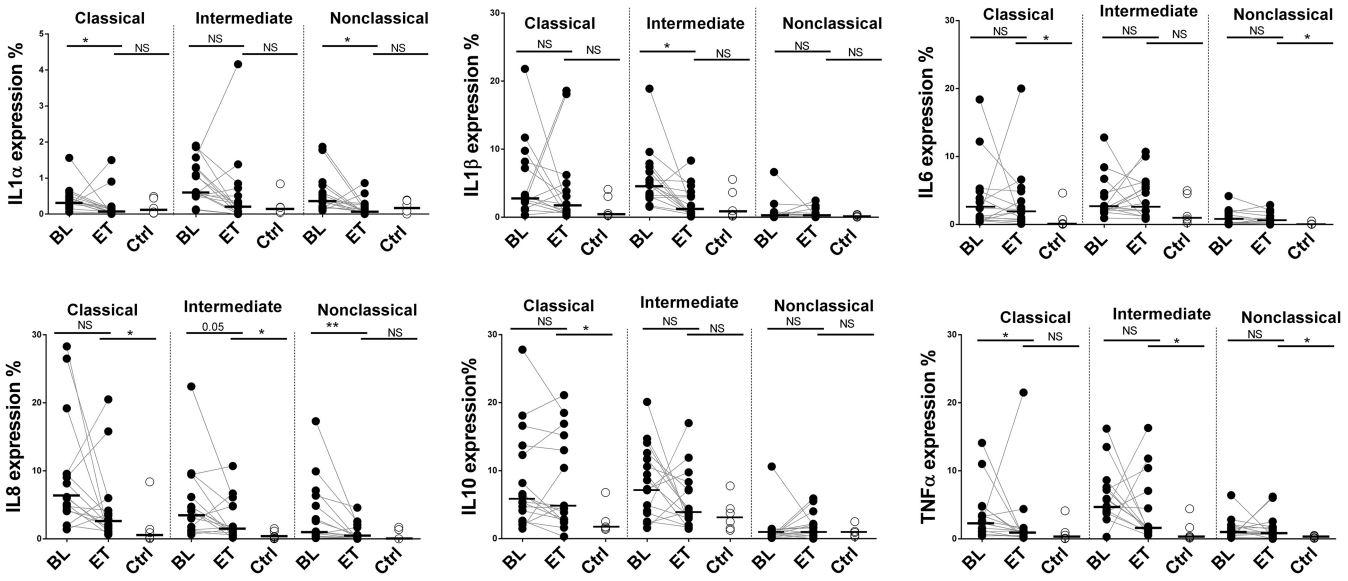


**FIG 3** Single-cytokine production. Shown are the percentages of classical, intermediate, and nonclassical monocytes producing IL-1$\alpha$, IL-1$\beta$, IL-6, IL-8, IL-10, and TNF-$\alpha$ after LPS stimulation. *, $P < 0.05$; **, $P < 0.001$; NS, not significant.

(Fig. 3). In summary, not all single cytokines reached the levels in HIV-monoinfected subjects in the different monocyte subsets.

**Polyfunctionality levels of monocytes in response to LPS after HCV eradication.** Polyfunctionality, understood as the simultaneous production of IL-1$\alpha$, IL-1$\beta$, IL-6, IL-8, IL-10, and TNF-$\alpha$ per monocyte subset after LPS stimulation, was studied before and after DAA treatment. The polyfunctionality index (Pindex) was decreased in the intermediate and nonclassical subsets after HCV clearance; however, it was remarkably increased compared to the HIV-monoinfected control group for all monocyte subsets after treatment (Fig. 4A). In addition, we observed a positive correlation between Pindex values and the percentages of classical, intermediate, and nonclassical monocytes expressing the costimulatory molecule CD40, associated with CVD (15), at baseline (rho = 0.430 and $P = 0.046$, rho = 0.554 and $P = 0.007$, and rho = 0.605 and $P = 0.003$, respectively). These direct correlations were not observed either at the end of treatment or in the HIV-monoinfected control group (Fig. 4B).

We also analyzed the 63 possible multiple-cytokine combinations after HCV clearance compared to the HIV-monoinfected control group in the three monocyte subsets (Table S2). Although, overall, we did not observe differences in Pindex values after treatment for the classical subset, reductions in several cytokine expression combinations including 6, 5, and 4 functions were detected after treatment, achieving the levels in the control group (Fig. 5A). However, at the same time, the classical subset was the one showing more differences at the end of treatment than in the control group (Table S2). For the IL-1$\alpha^-$ (IL-1$\alpha$-negative) IL-1$\beta^-$ IL-6$^+$ (IL-6-producing) IL-8$^-$ TNF-$\alpha^-$ IL-10$^-$ combination, this difference at the end of treatment compared to the control group occurred in all monocyte subsets after LPS stimulation (Fig. 5B).

**Cellular HIV-associated DNA after DAA therapy.** Cell-associated HIV-1 DNA was quite stable over time in the HIV/HCV-coinfected group receiving DAA treatment. Although we did not observe a difference before and after HCV clearance ($P = 0.622$), the HIV DNA level was significantly lower in the HIV/HCV-coinfected group than in the HIV-monoinfected group after DAA treatment (Fig. 6). Interestingly, a positive correlation was observed between HIV DNA and some inflammatory and activation biomarkers at the baseline: classical monocyte CD40 expression, intermediate monocyte CCR5 expression, and nonclassical monocyte CCR5 and CD11b expression (Fig. 7). These correlations were not observed at the end of treatment (Fig. S4).

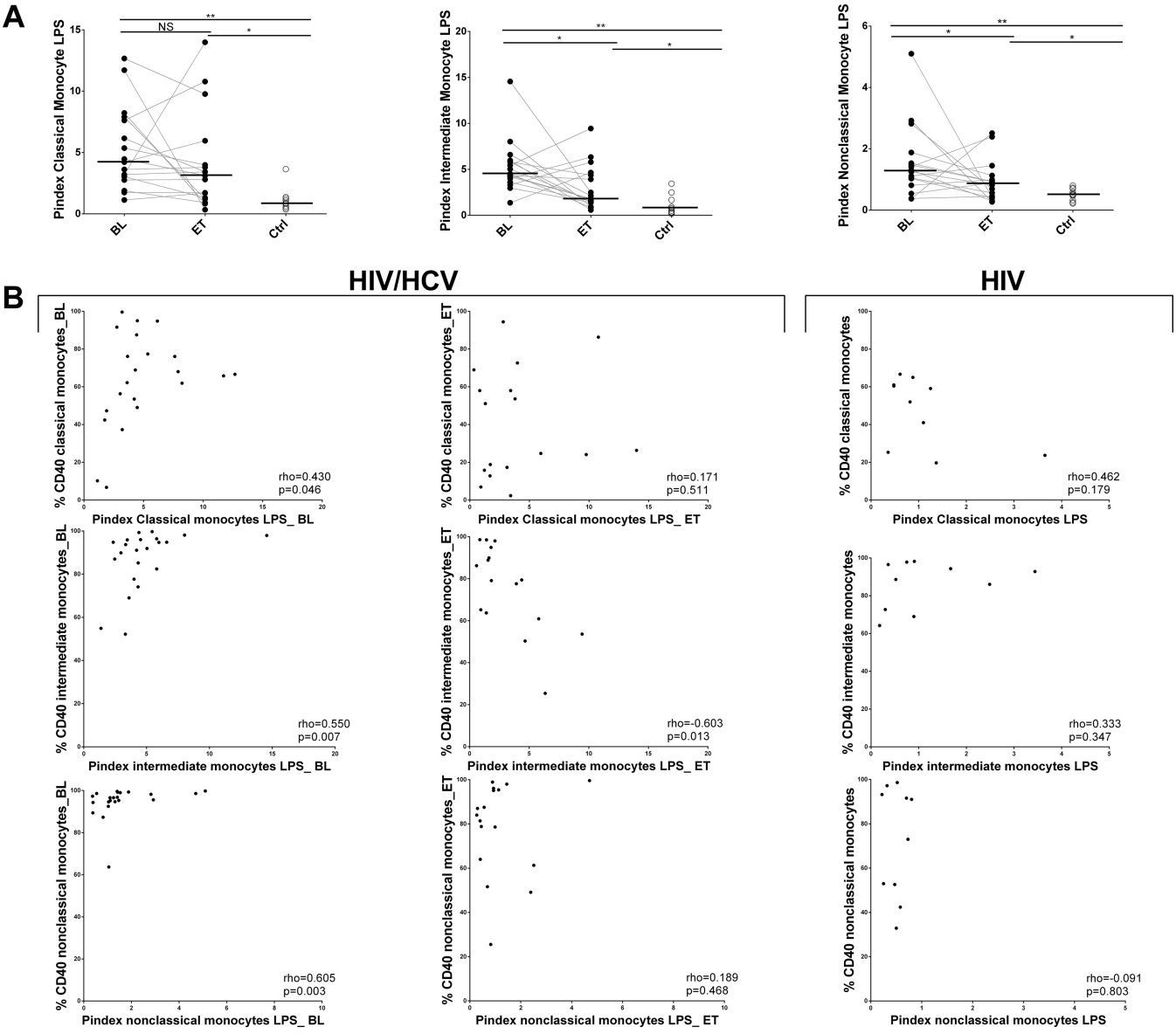


**FIG 4** Polyfunctionality of monocyte subsets after LPS stimulations. Polyfunctionality, understood as the simultaneous production of IL-1$\alpha$, IL-1$\beta$, IL-6, IL-8, IL-10, and TNF-$\alpha$ by classical, intermediate, and nonclassical monocytes, was studied before and after DAA therapy and in the HIV-monoinfected control group (Ctrl). (A) Polyfunctionality index values of classical, intermediate, and nonclassical monocytes after LPS stimulation. The Pindex was significantly higher in the HIV/HCV-coinfected group after DAA therapy than in the HIV-monoinfected control group. The Wilcoxon test was used to compare HIV/HCV-coinfected patients at baseline (BL) and at the end of treatment (ET). The Mann-Whitney U test was used to compare HIV/HCV-coinfected patients and the HIV-monoinfected patient control group. *, $P < 0.05$; **, $P < 0.001$; NS, not significant. (B) Graphical representation of the relationship between the Pindex and the percentage of monocytes expressing CD40 before and after DAA treatment and in the HIV-monoinfected control group. The Spearman correlation coefficient test was used.

## DISCUSSION

In the present study, we demonstrate that DAA therapy modulates monocyte phenotypes and functions, achieving a redistribution of monocyte subsets to a less proinflammatory profile and decreased monocyte activation and polyfunctionality. However, some specific features remained elevated compared to those in HIV-monoinfected subjects.

HIV/HCV coinfection induces immune dysfunctions that increase immune activation to levels higher than those in HIV-monoinfected subjects. This might explain the increased liver inflammation and fibrosis and the higher risk of cardiovascular events in coinfected patients (16, 17). We previously showed that HCV eradication reduced the immune activation of $CD4^+$ and $CD8^+$ T cells and soluble biomarkers associated with

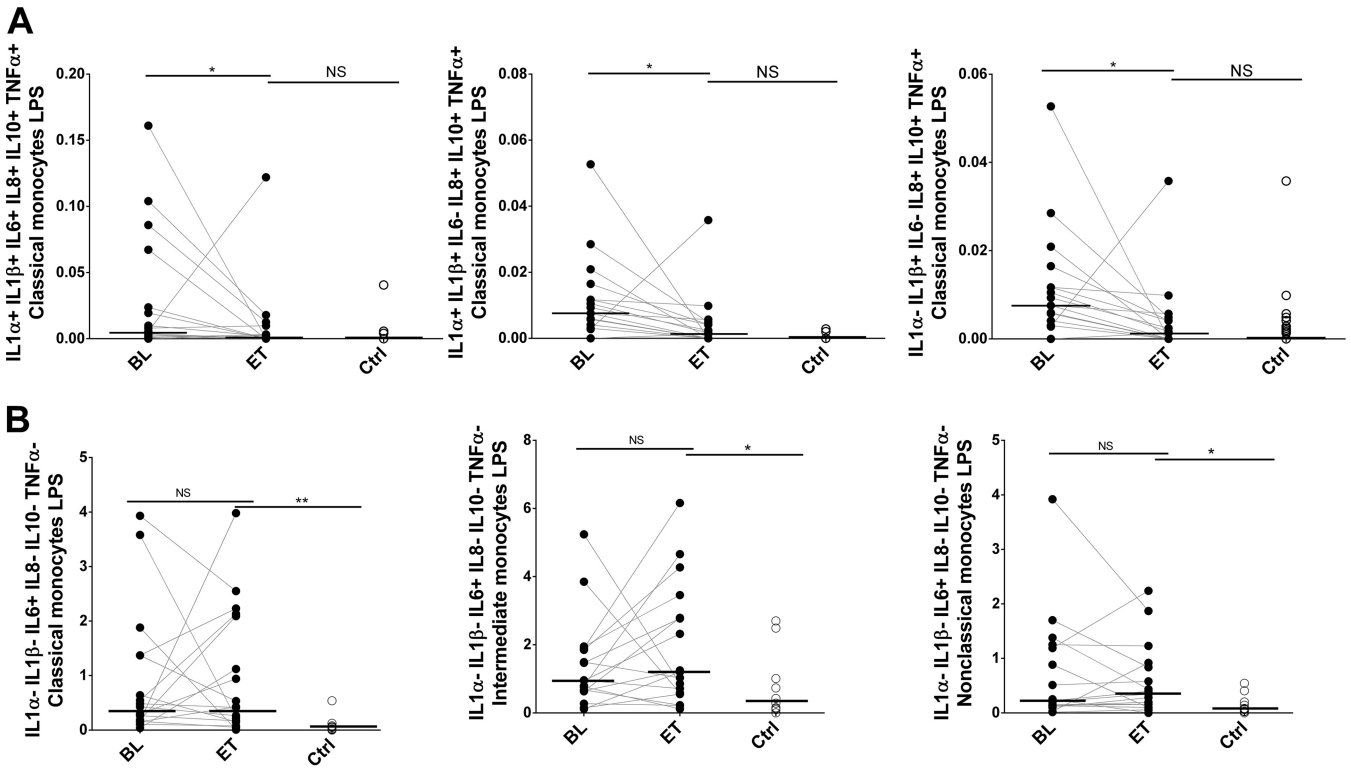


**FIG 5** Cytokine combinations produced by monocyte subsets in response to LPS. (A) Percentage of classical monocytes producing several combinations of cytokines after LPS stimulation. (B) IL-1$\alpha^-$ IL-1$\beta^-$ IL-6$^+$ IL-8$^-$ IL-10$^-$ TNF-$\alpha^-$ levels were significantly higher after DAA therapy in the three subsets than in the control group. The Wilcoxon test was used to compare HIV/HCV-coinfected patients at baseline (BL) and at the end of treatment (ET). The Mann-Whitney U test was used to compare HIV/HCV-coinfected patients and the HIV-monoinfected patient control group (Ctrl). *, $P < 0.05$; **, $P < 0.001$; NS, not significant.

innate immunity activation (11). Monocytes have been proposed to be the source of these biomarkers; therefore, it is important to know whether DAAs reduce monocyte activation and proinflammatory function. This is important since soluble markers of inflammation but not T cell activation have been associated with non-AIDS events in

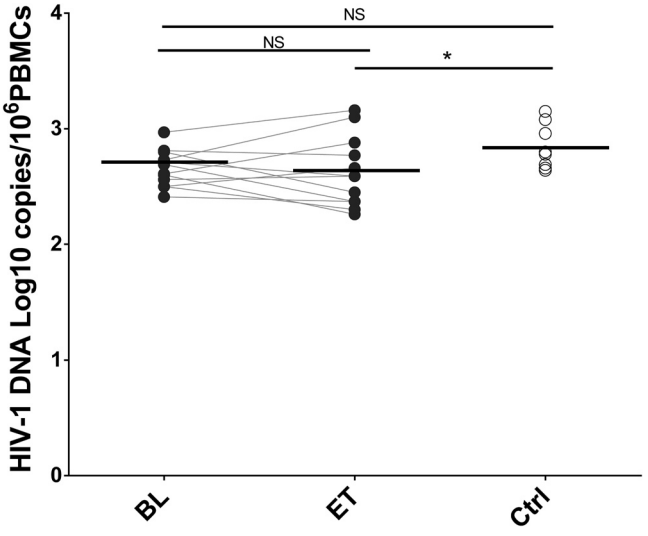


**FIG 6** Cell-associated HIV-1 DNA levels before and after DAA treatment. The Wilcoxon test was used to compare HIV/HCV-coinfected patients at baseline (BL) and at the end of treatment (ET). The Mann-Whitney U test was used to compare HIV/HCV-coinfected patients and the HIV-monoinfected patient control group (Ctrl). *, $P < 0.05$; NS, not significant.

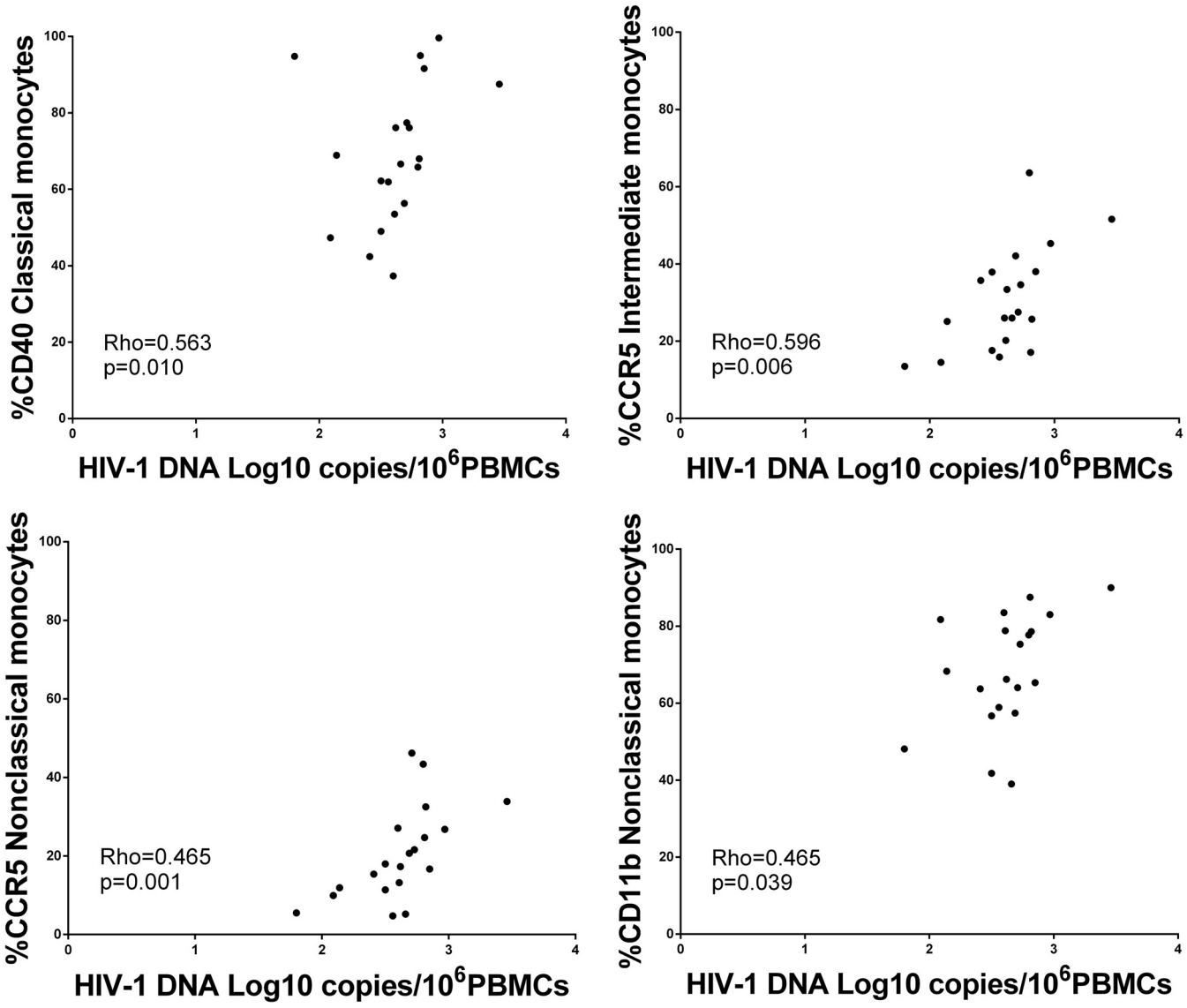


**FIG 7** Association of cell-associated HIV-1 DNA levels with the activation of monocytes before treatment. Shown is a graphical representation of the relationship between HIV-1 DNA $\log_{10}$ copies/$10^6$ PBMCs and the percentage of monocytes expressing CD40, CCR5, and CD11b before DAA treatment. The Spearman correlation coefficient test was used.

HIV-infected patients (18, 19). First, we observed a redistribution of monocyte subsets to a less proinflammatory profile, in accordance with recently reported data on HIV/HCV-coinfected patients (20). G. Ning et al. found similar results in HCV monoinfection in relation to healthy donors (13). These changes are important in terms of the reduction of cardiovascular risk since $CD16^+$ monocytes have been associated with these events in HCV-monoinfected and -coinfected patients (7, 8). In addition, HCV clearance produced decreases in several surface activation markers. Reductions in CD49d, CD40, and CX3CR1 expression and an increase in CD62L expression were observed. This profile resembled a reversion of the immunosenescence phenotype that occurs with chronological aging in monocytes (14, 21). These results indicate that, in this scenario, HCV infection induces an additional immunosenescence profile in HIV infection.

The decrease in monocyte activation came with improvements in the levels of soluble biomarkers. The levels of sCD163 decreased after DAA therapy, and no differences compared to HIV-monoinfected patients were observed; this is in accordance

with other studies of HIV-coinfected and HCV-monoinfected patients (12, 22, 23). This points toward decreased macrophage activation in the liver, as CD163 is a cell surface glycoprotein receptor that is highly expressed on most tissue macrophages, including hepatic Kupffer cells, and is cleaved from the cell surface in response to LPS, thus increasing the levels of the shed form of sCD163 in serum (23, 24). This improvement has been associated with a regression of liver fibrosis (25). In addition, it is important to mention that high levels of sCD163 have been associated with all-cause mortality in HIV infection (26). The same happened with the D-dimer and $\beta$2-microglobulin soluble biomarkers associated with all-cause mortality in HIV infection (27). This improvement in markers of coagulopathy such as D-dimers is in accordance with the decreases in monocyte activation mentioned above and with other work showing the beneficial effects of DAA treatment on vascular endothelial function (28). All these results highlight the favorable extrahepatic effects of eradicating HCV, especially in diminishing the risk of cardiovascular diseases or, as recently reported, improving cognitive impairment (20).

An approach to analyzing monocyte functionality is to characterize the production of single and multiple intracellular cytokines by monocytes. The production of multiple intracellular cytokines is known as polyfunctionality (9, 14), in this case after LPS stimulation. In general, according to phenotype results, we found a decrease in polyfunctionality with LPS stimulation after DAA therapy, with most of the cytokine combinations being decreased (cytokine combinations and polyfunctional index [Pindex]). However, Pindex values did not reach the levels in monoinfected patients for any monocyte subset. There were cytokine combinations, including the expression of only IL-6, TNF-$\alpha$, and IL-10, that were elevated in the three monocyte subsets compared to those in monoinfected patients after DAA treatment. These results were in accordance with those for single-cytokine production, where IL-6, TNF-$\alpha$, and IL-10 levels remained elevated in the different subsets. This cytokine signature is in accordance with the monocyte dysregulation of HIV-monoinfected patients compared to age-matched healthy controls with high levels of IL-6 and IL-10 (9). In this study, we show that this profile is exacerbated even after HCV eradication. This cytokine profile is remarkable as plasma IL-6 levels have been considered a powerful predictive parameter of the evolution of HIV infection, due to both AIDS- and non-AIDS-related entities (29, 30), although we did not find changes in the plasma levels of this cytokine.

We also examined the changes in cellular HIV DNA. We found no decrease after DAA therapy. However, in a previous study, we found a decrease in cell-associated HIV DNA after HCV eradication (11). This discrepancy is in accordance with contradictory results in the literature (11, 12, 31). It is known that the reservoir of proviral HIV-1 is enhanced in HCV/HIV-coinfected in comparison to HIV-monoinfected patients (32). This enhanced reservoir is presumably due to increased immune activation, including higher levels of liver inflammation, which are translated in heightened levels of fibrosis. Hence, this inconsistency may account for the different levels of inflammation and immune activation in the populations studied. In our previous analysis (11), there were higher levels of cirrhosis than in this study cohort. This may explain the higher levels of cell-associated HIV DNA before DAA therapy in populations with higher levels of activation, which would have a wide margin to decrease after immune activation is ameliorated due to DAAs. On the contrary, populations with low inflammation levels will also have low levels of cell-associated DNA, as is the case for the individuals in the extended study. In fact, at the end of DAA therapy, these subjects had even lower levels than those in HIV-monoinfected patients. However, it is noteworthy to mention that some effect was exerted by DAAs in the HIV reservoir because the association of cell-associated HIV DNA with some parameters of monocyte activation was observed only before treatment but not at the end of treatment. These associations are suggestive of a relationship between monocyte activation and the preservation of the HIV reservoir under conditions of high immune activation, such as HCV coinfection.

This study has several limitations. There were no time points studied after the end of treatment, so we do not know whether the remaining defects will disappear after a

longer follow-up. In addition, we do not know whether the low level of monocyte activation after treatment reaches the levels in the non-HIV/HCV-infected population. Previously, we found differences in monocyte activation and function between age-matched HIV-monoinfected subjects and healthy donor subjects (9). It is expected that the absence of complete normalization of monocyte activation and function parameters in HIV/HCV-coinfected patients after HCV eradication compared to HIV-monoinfected patients would also make differences compared with a healthy donor control group. However, these questions were not included in the design of the study, which was planned to observe the modulation of monocyte function and activation during DAA therapy. This study was restricted to patients with low levels of fibrosis. However, even in this population, decreases in monocyte activation were observed.

In conclusion, HCV clearance after DAA treatment in patients on successful suppressive cART exerts an anti-inflammatory profile on monocyte subsets and activation phenotypes. However, there is not a complete normalization of all parameters compared with HIV-monoinfected patients. These results may explain the deleterious effect of HCV infection on inflammation and the important implication of HCV elimination to ameliorate the development of non-AIDS events in patients on suppressive cART.

## MATERIALS AND METHODS

**Study subjects.** Patients who consecutively visited the Infectious Diseases Unit at the Virgen del Rocío University Hospital (Seville, Spain) from September 2017 to April 2018 were included if they fulfilled the following inclusion criteria: HIV/HCV-coinfected patients with detectable RNA for HCV and on cART with undetectable HIV RNA levels during the last 6 months. The included subjects achieved a sustained virological response (SVR) after 12 weeks of HCV treatment with DAAs; SVR was defined as a negative plasma HCV RNA test result 3 to 6 months after finishing anti-HCV therapy. Patients were treated under routine clinical care conditions, according to the prevalent HCV treatment guidelines at the time and the best medical judgment, based on HCV genotype, history of HCV treatment, drug interactions with cART, and liver fibrosis assessed by transient elastography (FibroScan; Echosens, Paris, France). Cirrhosis was defined as a liver stiffness value of $\geq$14.5 kPa (33). The exclusion criteria were hepatitis B virus coinfection, other concomitant causes of liver disease, active infections, and past or present treatment with steroids or immunosuppressive drugs before the start of anti-HCV therapy. Twenty-two HIV/HCV-coinfected patients on suppressive cART were included, using fresh samples. As a control group, fresh samples of 10 age-matched HIV-monoinfected patients on suppressive cART were also included. We also included a confirmatory cohort with 18 HIV/HCV-coinfected patients with frozen peripheral blood mononuclear cells (PBMCs) available just before (baseline) and after treatment with DAAs recruited from April to December 2015. The study was approved by the Ethics Committee of the Virgen del Rocio University Hospital (protocol code UCE-VHC-2015-1; internal code 1050-N-15), and all of the patients provided informed consent.

**Laboratory methods.** Absolute $CD4^+$ and $CD8^+$ T cell counts were measured at baseline and at the end of DAA treatment using an FC500 flow cytometer (Beckman-Coulter, Brea, CA). The plasma HIV-1 RNA concentration was measured using quantitative PCR (Cobas AmpliPrep/Cobas TaqMan HIV-1 test; Roche Molecular Systems, Basel, Switzerland) (lower detection limit, 20 HIV-1 RNA copies/ml) according to the manufacturer's protocol. The HCV RNA level was measured at baseline and at the end of DAA treatment using quantitative PCR assays (Cobas TaqMan test; Roche Diagnostic Systems, Pleasanton, CA) (detection limit, 15 IU/ml).

**Immunophenotyping and intracellular cytokine staining of monocytes.** The methods for immunophenotyping and intracellular cytokine staining of monocytes were previously described in detail (14). In this case, for the confirmatory cohort study ($n = 18$), we used frozen PBMCs, and after thawing, the cells were immediately immunophenotyped, as detailed below; *in vitro* polyfunctional assays cannot be accurately performed on frozen samples and were performed on the main cohort. Therefore, for the main cohort ($n = 22$), we used 1 ml of fresh whole-blood samples for immunophenotyping; these samples were collected in EDTA-lined tubes. Erythrocytes were lysed according to the manufacturer's instructions (lyse buffer; R&D, San Diego, CA), and the cells were immediately immunophenotyped using a panel of antibodies to determine lineage, activation, and the following cell adhesion surface markers and viability dye to exclude nonviable cells: Live/Dead fixable violet dead-cell stain, CD11b (Alexa Fluor 700 [AF700]), CD40 (allophycocyanin [APC]), CCR5 (allophycocyanin H7 [APCH7]), CD49d (fluorescein isothiocyanate [FITC]), TLR4 (brilliant violet [BV786]), CD62L (phycoerythrin [PE]), CD163 (phycoerythrin-cyanine 7 [PC7]), CD16 (phycoerythrin Texas Red [PETXRED]), CCR2 (BV605), CD14 (BV650), CX3CR1 (peridinin chlorophyll protein [PerCP]), HLA-DR (BV711), and CD19, CD3, and CD56 (BV510).

*In vitro* polyfunctional assays were performed on 1.5 ml of fresh whole-blood specimens that were collected in EDTA-lined tubes (extended-phase study). Erythrocytes were lysed as described above. Next, the cells were resuspended in R10 medium (RPMI 1640 medium supplemented with 10% heat-inactivated calf serum, 100 U/ml penicillin G, 100 $\mu$l/ml streptomycin sulfate, and 1.7 mM sodium glutamine) that contained 10 U/ml DNase I (Roche Diagnostics, Mannheim, Germany) and rested for 1 h. Cells were then stimulated with or without 0.05 ng/ml lipopolysaccharide (LPS) for 6 h *in vitro*, in the presence of 1 $\mu$g/ml anti-CD28, 1 $\mu$g/ml anti-CD49d (BD Biosciences, Franklin Lakes, NJ), and 10 $\mu$g/ml

brefeldin A (BioLegend, San Diego, CA), at 37°C with 5% $CO_2$. After a 6-h culture, monocyte activation and intracellular cytokine production were analyzed by multiparametric flow cytometry. Surface and intracellular staining for cytokine production was performed using the following antibody panel: TNF-$\alpha$ (AF700), IL-1$\alpha$ (FITC), IL-1$\beta$ (APC), CCR5 (APCH7), TLR4 (BV786), IL-6 (PE), IL-10 (PC7), CD16 (PETXRED), CCR2 (BV605), CD14 (BV650), IL-8 (PerCP), HLA-DR (BV711), and CD19, CD3, and CD56 (BV510). The responsiveness of *in vitro* cells was calculated by subtracting the results under unstimulated conditions. Multiparametric flow cytometry was performed using an LSR Fortessa cell analyzer (BD Biosciences), and minima of 2,000,000 total events and 20,000 monocytes were recorded for each tube (for the gating strategy, see Fig. S1B in the supplemental material). Data were analyzed using FlowJo 8.7.7 (TreeStar, San Carlos, CA, USA).

**Assay of soluble biomarkers.** Serum and plasma samples were collected in serum separation tubes and EDTA-lined tubes, respectively. The samples were aliquoted and stored at −20°C until subsequent analysis of the following biomarkers: high-sensitivity C-reactive protein (hsCRP), $\beta$2-microglobulin ($\beta$2M), D-dimer, IL-6, TNF-$\alpha$, and soluble CD163 (sCD163). The levels of hsCRP and $\beta$2M were determined by an immunoturbidimetric serum assay using a Cobas 701 analyzer (Roche Diagnostics, Mannheim, Germany). The D-dimer levels were measured by an automated latex-enhanced immunoassay using plasma samples (HemosIL D-dimer HS 500; Instrumentation Laboratory, Bedford, MA). IL-6, TNF-$\alpha$, and sCD163 plasma levels were determined by enzyme-linked immunoassays (ELISAs) (high sensitivity [R&D Systems, Minneapolis, MN] for IL-6 and TNF-$\alpha$ and Macro CD163 [IQproducts, The Netherlands] for sCD163) according to the manufacturers' instructions.

**Cellular HIV DNA quantification.** Levels of total HIV DNA were quantified from extracted DNA by droplet digital PCR (ddPCR) using the Bio-Rad QX200 droplet reader. Genomic DNA was extracted using a blood DNA minikit (Omega; Bio-Tek) according to the manufacturer's protocol. DNAs were treated with the BsaJI restriction enzyme (New England BioLabs [NEB]), according to the manufacturer's protocol, in preparation for ddPCR. DNA concentrations were measured using the Qubit assay (Thermo Fisher Scientific) and carried to a concentration of 30 ng/$\mu$l. The Bio-Rad QX200 ddPCR system was run according to the manufacturer's protocol, using an annealing temperature of 58°C. To circumvent sequence mismatches in viral sequences and for higher sensitivity, the following two primer sets in the viral 5′ long terminal repeat (LTR) and *gag* regions and probes were employed: primers 6F (5′-CATGTT TTCAGCATTATCAGAAGGA-3′) and 84R (5′-TGCTTGATGTCCCCCCACT-3′) and probe 5′-VIC-CCACCCCAC AAGATTTAAACACCATGCTAA-BHQ1 (black hole quencher 1)-3′ (34) as well as primers LT forward (5′-TGTGTGCCCGTCTGTTGTGT-3′) and LT reverse (5′-GCCGAGRCCTGCGTCGAGAG-3′) and the LT probe (5′-FAM [6-carboxyfluorescein]-CAGTGGCGCCCGAACAGGGA-BHQ1-3′) (35). The RPP30 gene was the host cell gene used to normalize HIV copies to 1 million cells with the following primers and probe: RPP30 forward (5′-GATTTGGACCTGCGAGCG-3′), RPP30 reverse (5′-GCGGCTGTCTCCACAAGT-3′), and probe 5′-VIC-CTGACCTGAAGGCTCT-BHQ1-3′ (36). Copy numbers were calculated using Bio-Rad QuantaSoft software v.1.7.4.

**Statistical analysis.** Continuous variables were expressed as medians and interquartile ranges (IQRs), and categorical variables were expressed as numbers and percentages. The chi-square and Mann-Whitney U tests were used to analyze differences between groups, and Wilcoxon tests were used to analyze differences throughout the treatment. Correlations between variables were assessed using Spearman's rank test. All $P$ values of $<0.05$ were considered significant. Statistical analysis was performed using Statistical Package for the Social Sciences software (SPSS 22.0; SPSS, Chicago, IL, USA). A total of 63 cytokine combinations were constructed using Pestle version 1.6.2 and Spice version 5.2 (provided by M. Roederer, NIH, Bethesda, MD) and quantified with the polyfunctionality index algorithm (Pindex) employing the 0.1.2 beta version of FunkyCells Boolean Dataminer software, provided by Martin Larson (INSERM U1135, Paris, France).

## SUPPLEMENTAL MATERIAL

Supplemental material is available online only.

**SUPPLEMENTAL FILE 1**, PDF file, 0.9 MB.

## ACKNOWLEDGMENTS

This study would not have been possible without the collaboration of all of the patients, medical and nursing staff, and data managers who have taken part in this project.

This work was supported by the Instituto de Salud Carlos III (research contracts CPII014/00025 to E.R.-M., CP19/00159 to A.G.-V., FI17/00186 to M.R.J.-L., and FI14/00431 to L.T.-D. and research projects PI16/00684 and PI19/01127 to E.R.-M.) and the Red Temática de Investigación Cooperativa en SIDA (RD16/0025/0020 and RD16/0025/0019), which is included in the Acción Estratégica en Salud, Plan Nacional de Investigación Científica, Desarrollo e Innovación Tecnológica, 2008 to 2011 and 2013 to 2016, Instituto de Salud Carlos III, Fondos FEDER. E.R.-M. was supported by the Consejería de Salud y Bienestar Social of the Junta de Andalucía through the Nicolás Monardes program (C-0032/17).

We declare that no conflicts of interest exist.

## REFERENCES


1. Abutaleb A, Sherman KE. 2018. A changing paradigm: management and treatment of the HCV/HIV-co-infected patient. Hepatol Int 12:500–509. https://doi.org/10.1007/s12072-018-9896-4.
2. Klein MB, Althoff KN, Jing Y, Lau B, Kitahata M, Lo Re V, III, Kirk GD, Hull M, Kim HN, Sebastiani G, Moodie EEM, Silverberg MJ, Sterling TR, Thorne JE, Cescon A, Napravnik S, Eron J, Gill MJ, Justice A, Peters MG, Goedert JJ, Mayor A, Thio CL, Cachay ER, Moore R, North American AIDS Cohort Collaboration on Research and Design of IeDEA. 2016. Risk of end-stage liver disease in HIV-viral hepatitis coinfected persons in North America from the early to modern antiretroviral therapy eras. Clin Infect Dis 63:1160–1167. https://doi.org/10.1093/cid/ciw531.
3. Sandler NG, Wand H, Roque A, Law M, Nason MC, Nixon DE, Pedersen C, Ruxrungtham K, Lewin SR, Emery S, Neaton JD, Brenchley JM, Deeks SG, Sereti I, Douek DC, INSIGHT SMART Study Group. 2011. Plasma levels of soluble CD14 independently predict mortality in HIV infection. J Infect Dis 203:780–790. https://doi.org/10.1093/infdis/jiq118.
4. Funderburg NT, Zidar DA, Shive C, Lioi A, Mudd J, Musselwhite LW, Simon DI, Costa MA, Rodriguez B, Sieg SF, Lederman MM. 2012. Shared monocyte subset phenotypes in HIV-1 infection and in uninfected subjects with acute coronary syndrome. Blood 120:4599–4608. https://doi.org/10.1182/blood-2012-05-433946.
5. Fernández-Montero JV, Barreiro P, De Mendoza C, Labarga P, Soriano V. 2016. Hepatitis C virus coinfection independently increases the risk of cardiovascular disease in HIV-positive patients. J Viral Hepat 23:47–52. https://doi.org/10.1111/jvh.12447.
6. Cros J, Cagnard N, Woollard K, Patey N, Zhang S-Y, Senechal B, Puel A, Biswas SK, Moshous D, Picard C, Jais J-P, D'Cruz D, Casanova J-L, Trouillet C, Geissmann F. 2010. Human CD14 dim monocytes patrol and sense nucleic acids and viruses via TLR7 and TLR8 receptors. Immunity 33:375–386. https://doi.org/10.1016/j.immuni.2010.08.012.
7. Rogacev KS, Cremers B, Zawada AM, Seiler S, Binder N, Ege P, Große-Dunker G, Heisel I, Hornof F, Jeken J, Rebling NM, Ulrich C, Scheller B, Böhm M, Fliser D, Heine GH. 2012. CD14++CD16+ monocytes independently predict cardiovascular events: a cohort study of 951 patients referred for elective coronary angiography. J Am Coll Cardiol 60:1512–1520. https://doi.org/10.1016/j.jacc.2012.07.019.
8. Baker JV, Hullsiek KH, Singh A, Wilson E, Henry K, Lichtenstein K, Onen N, Kojic E, Patel P, Brooks JT, Hodis HN, Budoff M, Sereti I, CDC SUN Study Investigators. 2014. Immunologic predictors of coronary artery calcium progression in a contemporary HIV cohort. AIDS 28:831–840. https://doi.org/10.1097/QAD.0000000000000145.
9. De Pablo-Bernal RS, Ramos R, Genebat M, Cañizares J, Rafii-El-Idrissi Benhnia M, Muñoz-Fernández MA, Pacheco YM, Galvá MI, Leal M, Ruiz-Mateos E. 2016. Phenotype and polyfunctional deregulation involving interleukin 6 (IL-6)- and IL-10-producing monocytes in HIV-infected patients receiving combination antiretroviral therapy differ from those in healthy older individuals. J Infect Dis 213:999–1007. https://doi.org/10.1093/infdis/jiv520.
10. Lidofsky A, Holmes JA, Feeney ER, Kruger AJ, Salloum S, Zheng H, Seguin IS, Altinbas A, Masia R, Corey KE, Gustafson JL, Schaefer EA, Hunt PW, Deeks S, Somsouk M, Chew KW, Chung RT, Alatrakchi N. 2018. Macrophage activation marker soluble CD163 is a dynamic marker of liver fibrogenesis in human immunodeficiency virus/hepatitis C virus coinfection. J Infect Dis 218:1394–1403. https://doi.org/10.1093/infdis/jiy331.
11. López-Cortés LF, Trujillo-Rodríguez M, Báez-Palomo A, Benmarzouk-Hidalgo OJ, Dominguez-Molina B, Milanés-Guisado Y, Espinosa N, Viciana P, Gutiérrez-Valencia A. 2018. Eradication of hepatitis C virus (HCV) reduces immune activation, microbial translocation, and the HIV DNA level in HIV/HCV-coinfected patients. J Infect Dis 218:624–632. https://doi.org/10.1093/infdis/jiy136.
12. Parisi SG, Andreis S, Mengoli C, Menegotto N, Cavinato S, Scaggiante R, Andreoni M, Palù G, Basso M, Cattelan AM. 2018. Soluble CD163 and soluble CD14 plasma levels but not cellular HIV-DNA decrease during successful interferon-free anti-HCV therapy in HIV-1-HCV co-infected patients on effective combined anti-HIV treatment. Med Microbiol Immunol 207:183–194. https://doi.org/10.1007/s00430-018-0538-1.
13. Ning G, Li YT, Chen YM, Zhang Y, Zeng YF, Lin CS. 2017. Dynamic changes of the frequency of classic and inflammatory monocytes subsets and natural killer cells in chronic hepatitis C patients treated by direct-acting antiviral agents. Can J Gastroenterol Hepatol 2017:3612403. https://doi.org/10.1155/2017/3612403.
14. de Pablo-Bernal RS, Cañizares J, Rosado I, Galvá MI, Alvarez-Ríos AI, Carrillo-Vico A, Ferrando-Martínez S, Muñoz-Fernández MÁ, Rafii-El-Idrissi Benhnia M, Pacheco YM, Ramos R, Leal M, Ruiz-Mateos E. 2016. Monocyte phenotype and polyfunctionality are associated with elevated soluble inflammatory markers, cytomegalovirus infection, and functional and cognitive decline in elderly adults. J Gerontol A Biol Sci Med Sci 71:610–618. https://doi.org/10.1093/gerona/glv121.
15. Tarancon-Diez L, de Pablo-Bernal RS, Alvarez-Ríos AI, Rosado-Sánchez I, Dominguez-Molina B, Genebat M, Pacheco YM, Jiménez JL, Ángeles Muñoz-Fernández M, Ruiz-Mateos E, Leal M. 2017. CCR5+ CD8 T-cell levels and monocyte activation precede the onset of acute coronary syndrome in HIV-infected patients on antiretroviral therapy. Thromb Haemost 117:1141–1149. https://doi.org/10.1160/TH16-11-0867.
16. Chen JY, Feeney ER, Chung RT. 2014. HCV and HIV co-infection: mechanisms and management. Nat Rev Gastroenterol Hepatol 11:362–371. https://doi.org/10.1038/nrgastro.2014.17.
17. Genebat M, Tarancón-Díez L, Pulido I, Álvarez-Ríos AI, Muñoz-Fernández MÁ, Ruiz-Mateos E, Leal M. 2019. Hepatitis C virus and cumulative infections are associated with atherogenic cardiovascular events in HIV-infected subjects. Antiviral Res 169:104527. https://doi.org/10.1016/j.antiviral.2019.05.016.
18. Tenorio AR, Zheng Y, Bosch RJ, Krishnan S, Rodriguez B, Hunt PW, Plants J, Seth A, Wilson CC, Deeks SG, Lederman MM, Landay AL. 2014. Soluble markers of inflammation and coagulation but not T-cell activation predict non-AIDS-defining morbid events during suppressive antiretroviral treatment. J Infect Dis 210:1248–1259. https://doi.org/10.1093/infdis/jiu254.
19. Angelidou K, Hunt PW, Landay AL, Wilson CC, Rodriguez B, Deeks SG, Bosch RJ, Lederman MM. 2018. Changes in inflammation but not in T-cell activation precede non-AIDS-defining events in a case-control study of patients on long-term antiretroviral therapy. J Infect Dis 218:239–248. https://doi.org/10.1093/infdis/jix666.
20. Sun B, Abadjian L, Monto A, Freasier H, Pulliam L. 11 March 2020. HCV cure in HIV coinfection dampens inflammation and improves cognition through multiple mechanisms. J Infect Dis https://doi.org/10.1093/infdis/jiaa109.
21. Hearps AC, Maisa A, Cheng W-J, Angelovich TA, Lichtfuss GF, Palmer CS, Landay AL, Jaworowski A, Crowe SM. 2012. HIV infection induces age-related changes to monocytes and innate immune activation in young men that persist despite combination antiretroviral therapy. AIDS 26:843–853. https://doi.org/10.1097/QAD.0b013e328351f756.
22. Lund Laursen T, Brøckner Siggard C, Kazankov K, Damgaard Sandahl T, Møller HJ, Ong A, Douglas MW, George J, Tarp B, Hagelskjaer Kristensen L, Lund Laursen A, Hiramatsu A, Nakahara T, Chayama K, Grønbaek H. 2018. Rapid and persistent decline in soluble CD163 with successful direct-acting antiviral therapy and associations with chronic hepatitis C histology. Scand J Gastroenterol 53:986–993. https://doi.org/10.1080/00365521.2018.1481996.
23. Kostadinova L, Shive CL, Zebrowski E, Fuller B, Rife K, Hirsch A, Compan A, Moreland A, Falck-Ytter Y, Popkin DL, Anthony DD. 2018. Soluble markers of immune activation differentially normalize and selectively associate with improvement in AST, ALT, albumin, and transient elastography during IFN-free HCV therapy. Pathog Immun 3:438–444. https://doi.org/10.20411/pai.v3i1.242.
24. French AL, Martin JW, Evans CT, Peters M, Kessaye SG, Nowicki M, Kuniholm M, Golub E, Augenbraun M, Desai SN, WIHS. 2017. Macrophage activation and the tumor necrosis factor cascade in hepatitis C disease progression among HIV-infected women participating in the Women's Interagency HIV Study (WIHS). J Acquir Immune Defic Syndr 74:438–444. https://doi.org/10.1097/QAI.0000000000001524.
25. Laursen TL, Siggaard CB, Kazankov K, Sandahl TD, Møller HJ, Tarp B, Kristensen LH, Laursen AL, Leutscher P, Grønbæk H. 2020. Time-dependent improvement of liver inflammation, fibrosis and metabolic liver function after successful direct-acting antiviral therapy of chronic hepatitis C. J Viral Hepat 27:28–35. https://doi.org/10.1111/jvh.13204.
26. Knudsen TB, Ertner G, Petersen J, Møller HJ, Moestrup SK, Eugen-Olsen J, Kronborg G, Benfield T. 2016. Plasma soluble CD163 level independently predicts all-cause mortality in HIV-1-infected individuals. J Infect Dis 214:1198–1204. https://doi.org/10.1093/infdis/jiw263.
27. Dysangco A, Liu Z, Stein JH, Dubé MP, Gupta SK. 2017. HIV infection, antiretroviral therapy, and measures of endothelial function, inflamma-

tion, metabolism, and oxidative stress. PLoS One 12:e0183511. https://doi.org/10.1371/journal.pone.0183511.
28. Schmidt FP, Zimmermann T, Wenz T, Schnorbus B, Ostad MA, Feist C, Grambihler A, Schattenberg JM, Sprinzl MF, Münzel T, Galle PR. 2018. Interferon- and ribavirin-free therapy with new direct acting antivirals (DAA) for chronic hepatitis C improves vascular endothelial function. Int J Cardiol 271:296–300. https://doi.org/10.1016/j.ijcard.2018.04.058.
29. Boulware DR, Hullsiek KH, Puronen CE, Rupert A, Baker JV, French MA, Bohjanen PR, Novak RM, Neaton JD, Sereti I. 2011. Higher levels of CRP, D-dimer, IL-6, and hyaluronic acid before initiation of antiretroviral therapy (ART) are associated with increased risk of AIDS or death. J Infect Dis 203:1637–1646. https://doi.org/10.1093/infdis/jir134.
30. Sunil M, Nigalye M, Somasunderam A, Martinez ML, Yu X, Arduino RC, Utay NS, Bell TK. 2016. Unchanged levels of soluble CD14 and IL-6 over time predict serious non-AIDS events in HIV-1-infected people. AIDS Res Hum Retroviruses 32:1205–1209. https://doi.org/10.1089/AID.2016.0007.
31. Rozera G, Fabbri G, Lorenzini P, Mastrorosa I, Timelli L, Zaccarelli M, Amendola A, Vergori A, Plazzi MM, Cicalini S, Antinori A, Capobianchi MR, Abbate I, Ammassari A. 2017. Peripheral blood HIV-1 DNA dynamics in antiretroviral-treated HIV/HCV co-infected patients receiving directly-acting antivirals. PLoS One 12:e0187095. https://doi.org/10.1371/journal.pone.0187095.
32. López-Huertas MR, Palladino C, Garrido-Arquero M, Esteban-Cartelle B, Sánchez-Carrillo M, Martínez-Román P, Martín-Carbonero L, Ryan P, Domínguez-Domínguez L, De Los Santos I, De La Fuente Moral S, Benito JM, Rallón N, Alcamí J, Resino S, Fernández-Rodríguez A, Coiras M, Briz V, Multidisciplinary Group of Viral Coinfection HIV/Hepatitis. 2019. HCV-coinfection is related to an increased HIV-1 reservoir size in cART-treated HIV patients: a cross-sectional study. Nature 9:5606. https://doi.org/10.1038/s41598-019-41788-9.
33. Vergara S, Macías J, Rivero A, Gutiérrez-Valencia A, González-Serrano M, Merino D, Ríos MJ, García-García JA, Camacho A, López-Cortés L, Ruiz J, de la Torre J, Viciana P, Pineda JA, Grupo para el Estudio de las Hepatitis Víricas de la SAEI. 2007. The use of transient elastometry for assessing liver fibrosis in patients with HIV and hepatitis C virus coinfection. Clin Infect Dis 45:969–974. https://doi.org/10.1086/521857.
34. Palmer S, Wiegand AP, Maldarelli F, Bazmi H, Mican JM, Polis M, Dewar RL, Planta A, Liu S, Metcalf JA, Mellors JW, Coffin JM. 2003. New real-time reverse transcriptase-initiated PCR assay with single-copy sensitivity for human immunodeficiency virus type 1 RNA in plasma. J Clin Microbiol 41:4531–4536. https://doi.org/10.1128/JCM.41.10.4531-4536.2003.
35. Ishizaka A, Sato H, Nakamura H, Koga M, Kikuchi T, Hosoya N, Koibuchi T, Nomoto A, Kawana-Tachikawa A, Mizutani T. 2016. Short intracellular HIV-1 transcripts as biomarkers of residual immune activation in patients on antiretroviral therapy. J Virol 90:5665–5676. https://doi.org/10.1128/JVI.03158-15.
36. Strain MC, Lada SM, Luong T, Rought SE, Gianella S, Terry VH, Spina CA, Woelk CH, Richman DD. 2013. Highly precise measurement of HIV DNA by droplet digital PCR. PLoS One 8:e55943. https://doi.org/10.1371/journal.pone.0055943.